The role of magnesium for geometry and charge in GTP hydrolysis, revealed by QM/MM simulations

Till Rudack[*], *Fei Xia*[†], *Jürgen Schlitter* [*], *Carsten Kötting* [*] *and Klaus Gerwert* [*†]

[*] Department of Biophysics, Ruhr-University Bochum, Universitätsstraße 150, 44801 Bochum, Germany
[†] CAS–Max-Planck Partner Institute for Computational Biology (PICB), Shanghai Institutes for Biological Sciences (SIBS), 320 Yue Yang Road, 200031 Shanghai, P.R. China

Supporting Material

Molecular Mechanics Simulations

We deployed a combination of MM and QM/MM simulation (Fig. 1) to acquire charge shifts and structural details, which are validated by comparison of calculated spectral features with experimental ones. MM simulations are necessary for pre-equilibration and for creating different snapshots from an equilibrated MM trajectory, revealing protein fluctuations that are also mirrored in the FTIR spectra. The investigated simulation systems were: GTP; GTP·Mg^{2+}; Ras·GTP·Mg^{2+} (based on PDB-ID: 1QRA) (1); Ras·GTP·Mg^{2+}·RasGAP (PDB-ID: 1WQ1) (2); Ras·GDP·Mg^{2+}·Pi·RasGAP; and Ras·GDP·Mg^{2+} (PDB-ID: 4Q21) (3). Each simulation was carried out in a cubic box filled with water and salt at physiological concentration. Hydrogens were first added to the crystal structures. The structures were checked and amended with the MAXIMOBY algorithm (4). A detailed list of the composition of each simulation system is presented in Table S1. MM simulations were performed with GROMACS 4.0.7 (5, 6) using double precision (machine precision of $1.11 \cdot 10^{-16}$) and the OPLS/AA force field (7) with improved parameters for the tri- and diphosphate. Periodic boundary conditions were applied to the cubic box filled with Tip4p waters (8) and sodium and chloride ions at physiological concentrations. The van der Waals interactions between atom pairs were truncated with a cutoff value of 1.4 nm. The Fast Particle-Mesh Ewald method (9) with a grid spacing of 0.12 nm and fourth-order spline interpolation was used for evaluation of the electrostatic interactions of the system. The v-rescale algorithm (10) was used to separately couple the solute and the solvents (including the ions) to an external temperature bath with a time constant of 0.1 ps to keep the system at a constant temperature of 300 K. The Parinello-Rahman algorithm (11) with a coupling constant of 1.0 ps was used to couple the system to an isotropic pressure bath of 1 standard atmosphere. The system was first energy-minimized and then heated to 300 K. Next, 50 ns MM simulations were performed for each system. The coordinating contacts of the substrate with its surrounding were analyzed by the contact matrix algorithm of MAXIMOBY (4).

Quantum Mechanics/Molecular Mechanics simulations

After 25 ns of MM, each of the systems was equilibrated referring to the energy criteria of MAXIMOBY (4). We took six snapshots every 5 ns beginning after 25 ns of the MM trajectories. Following the approach of Fei *et al.* (12), these structures were equilibrated for 2.5 ps by the QM/MM interface GROMACS/G03 (6, 13, 14). The ribose, the triphosphate, and the Mg^{2+} were treated quantum mechanically with the B3LYP/6-31G* level of theory. Therefore, accurate normal vibrational modes of these atoms within the QM region can be obtained by diagonalizing the Hessian matrix after minimizing the selected QM atoms while fixing the MM region at the structure at 300 K. This method is called instantaneous normal mode analysis (INMA). For the INMA we used three different basis sets: 6-31G*,

6-31++G**, and 6-311++G**. The calculated vibrational modes were compared to the experimental values. From these validated structures, a 0.5 ps evaluation run with GROMACS/CPMD was initiated (6, 15, 16) [functional: Becke/Perdew (17, 18), pseudo-potential: Goedecker/Hartwigsen (19) with a cut-off of 80 Ry]. The triphosphate, the Mg^{2+}, and its coordinating partners were treated quantum mechanically for a precise analysis of these last 0.5 ps QM/MM trajectories regarding charge shifts and structural details.

Charge calculations
Charges were calculated every 0.25 fs using electrostatic potentials (ESP) (20). For each atom in the quantum region, we determined an average partial charge over the 2,000 values of the trajectory for one snapshot. The relative error of these values is about 10%. The value for each atom of one snapshot was then averaged over the six different snapshots. The standard deviation indicates the dependence of the partial charge on the structure. In the next step, the atoms were categorized into nine functional groups, and the partial charges were summed for each group (Fig. S5). The nine groups were: 1) the magnesium ion, 2) the γ-phosphate (consisting of the atoms: O_{13}, O_{23}, O_{33} and P_3), 3) the P_i (O_1, O_2, O_3, O_4, H_3, H_4 and $_P$) in the intermediate state, 4) the β-phosphate (O_{12}, O_{22}, O_{32}, O_{31} and P_2), 5) the α-phosphate (O_{11}, O_{21}, $O_{5'}$ and P_1), 6) the methyl group (H_5, $H_{5'}$, $H_{5''}$ and $C_{5'}$) where H_5 is a dummy atom at the junction between the QM and MM regions, 7) Ser17, 8) Thr35, and 9) the group HOH summarizing all coordinating water molecules. The coordinating partners, which depend on the analyzed state, are Ser17, Thr35, and two to four waters.

Structure calculations
All bond distances, bond angles, and dihedrals of the phosphate groups were calculated every 0.25 fs of the 500 fs QM/MM trajectory. For each of the six snapshots, we acquired 2,000 values. For each state, we averaged a total of over 12,000 values. In all states, one stable conformation was reached, indicated by a relative error of less than 1%.

Validation method
The frequencies of the triphosphate were calculated by INMA after 2.5 ps of QM/MM equilibration, based on the demonstration by Fei *et al.* (12) that, for the simulation systems analyzed herein, the calculated frequencies of several snapshots of a 100 ps trajectory differ only very slightly from the one after 2.5 ps. To validate the equilibrated structure, we compared nine normal vibrational modes of the triphosphate group of GTP with the available frequencies from FTIR measurements, which are assigned by isotopic labeling. For the diphosphate of GDP, seven vibrational modes were analyzed. As comparison criteria, we calculated the root-mean-square deviation (RMSD) between the calculated and measured frequencies.

The triphosphate group is composed of a $(PO_2)_\alpha$ group, a $(PO_2)_\beta$ group, and a dianionic $(PO_3)_\gamma$ group. The $(PO_2)_\alpha$ and $(PO_2)_\beta$ groups possess antisymmetric and symmetric stretching vibrational modes, denoted as $\nu_{a/s}(PO_2)_\alpha$ and $\nu_{a/s}(PO_2)_\beta$, respectively. Due to the coupling between the vibrational modes of $(PO_2)_\alpha$ and $(PO_2)_\beta$, we observed in-phase and out-of-phase vibrational modes according to Wang *et al.* (21) and Takeushi *et al.* (22), denoted as $\nu_{in}(PO_2)_{\alpha,\beta}$ and $\nu_{out}(PO_2)_{\alpha,\beta}$. The $(PO_3)_\gamma$ moiety has two antisymmetric vibrations, denoted as $\nu_a(PO_3)_\gamma$, and a symmetric vibration, $\nu_s(PO_3)_\gamma$. The symmetric $\nu_s(OP_\beta O)$ and the antisymmetric $\nu_a(OP_\beta O)$ stretching vibrations were analyzed as well. The diphosphate group is composed of a $(PO_2)_\alpha$ group and a dianionic $(PO_3)_\beta$ group. The $(PO_2)_\alpha$ group possesses an antisymmetric and a symmetric stretching vibrational mode, denoted as $\nu_{a/s}(PO_2)_\alpha$. The $(PO_3)_\beta$

moiety has two antisymmetric vibrations, denoted as $\nu_a(PO_3)_\beta$, and a symmetric vibration $\nu_s(PO_3)_\beta$. Furthermore the symmetric $\nu_s(OP_\alpha O)$ and the antisymmetric $\nu_a(OP_\alpha O)$ stretching vibrations were analyzed. To handle the coupling effects between some vibrational modes and make a clear-cut theoretical assignment, we estimated the contribution of each atom to the total vibration mode by calculating the percentage of the mass-weighted eigenvector of each atom to the total eigenvector.

Due to the highly flexible GTP structure in water, clear experimental band assignment of the vibration modes lying close to each other is very difficult. A broad infrared band at 1234 cm^{-1} has been observed for adenosine triphosphate (ATP) in water at pH 7.5, which has been attributed to the overlapping of the two vibration modes $\nu_a(PO_2)_\alpha$ and $\nu_a(PO_2)_\beta$. For GTP in water, Wang *et al.* (21) observed a similar broad band at 1233 cm^{-1}. The two modes $\nu_s(OP_\beta O)$ and $\nu_a(OP_\beta O)$ are not yet experimentally assigned for GTP in water. In total, five experimentally assigned vibrational modes from Wang *et al.* (21) are available for comparison. The magnesium ion stabilizes the triphosphate structure already in water (12). Takeuschi *et al.* (22) have differentiated the $\nu_a(PO_2)_\alpha$ and $\nu_a(PO_2)_\beta$ vibrational modes of ATP with bound Mg^{2+} in water, in contrast to Wang *et al.* (21), for GTP with bound Mg^{2+}. Therefore, we used the $\nu_a(PO_2)_\alpha$ and $\nu_a(PO_2)_\beta$ from Takeuschi *et al.* (22) for comparison, and assumed that the influence of the nucleoside on these vibrational modes is negligible. Together with the vibrational modes $\nu_{in}(PO_2)_{\alpha,\beta}$, $\nu_{out}(PO_2)_{\alpha,\beta}$, $\nu_a(PO_3)_\gamma$, and $\nu_s(PO_3)_\gamma$ for GTP with Mg^{2+} in water from Wang *et al.* (21), six experimentally assigned vibrational modes are available for comparison. For Ras·GTP·Mg^{2+} and Ras·GTP·Mg^{2+}·RasGAP, the experimental results of Allin *et al.* (23) are available for all nine vibrational modes. For Ras·GDP·Mg^{2+}, only three experimentally assigned vibrational modes $\nu_a(PO_2)_\alpha$, $\nu_a(PO_3)_\beta$ and $\nu_s(PO_3)_\beta$ by Allin *et al.* (23) are available for comparison.

We compared vibration modes not only to experimental results, but also to those derived by different theoretical methods. For the comparison, all nine vibrational modes were taken into account. The results for GTP in water (with and without Mg^{2+}) and for Ras·GTP·Mg^{2+} were compared to the results from Fei *et al.* (12). They used normal mode analysis (B3LYP/6-31G*) and selected the structure with vibrational modes that best fit the experiment. In contrast to this approach, which used only a single snapshot, we used INMA and averaged over six snapshots. We also compared different basis sets while using the same quantum region and the QM method used in Fei *et al.* (12). The vibration modes of the Ras·GTP·Mg^{2+} and the Ras·GTP·Mg^{2+}·RasGAP systems were compared to the theoretical results of te Heesen *et al.* (24), who averaged the normal vibration modes over six snapshots and used INMA. However, the six snapshots used herein encompass a much longer period (50 ns) of the MM trajectory than the 1 ns trajectory from a single snaphot from te Heesen *et al.* (24). This has improved our consideration of the role of protein motion. The quantum region of te Heesen *et al.* (24) only includes the triphosphate and not the ribose or the Mg^{2+}. Further, they used CPMD (15) instead of Gaussian03 (13) for the normal mode analysis.

Fei *et al.* (12) and te Heesen *et al* (24) calculated the RMSD of the vibrational modes of the triphosphate groups of Ras·GTP·Mg^{2+} to be 25 cm^{-1} and 34 cm^{-1}, respectively. Rudbeck *et al.* (25) reported an RMSD of 25 cm^{-1} for the vibrational modes of a fully ionized phosphoenol pyruvate. Our predicted RMSD of 24 cm^{-1} with 6-31++G** is consistent with these results. In general, an RMSD below 30 cm^{-1} (~2%) between the calculated and measured frequencies indicates good agreement.

Comparison of basis sets

We calculated all vibrational modes by INMA with the B3LYP function and tested three different basis sets: 6-31G*, 6-31++G**, and 6-311++G**. The RMSDs between experimentally assigned (26) and calculated values for the nine vibrational triphosphate modes for Ras·GTP·Mg^{2+} were 30 cm^{-1} with the basis set 6-31G*, 24 cm^{-1} with 6-31++G**, and 29 cm^{-1} with 6-311++G**. In general, the vibrational modes calculated with 6-31G* overestimate the experimental frequencies. The best results were reached by including the diffuse and polarization functions; an enlargement of the basis set did not lead to further optimization. This is consistent with the observations of Rudbeck *et al.* (25), who also calculated vibrational modes of phophate groups. The results are comparable for all analyzed systems. Therefore, we describe here only the results for the INMA with B3LYP/6-31++G**. Detailed values of the average over the six snapshots for each vibrational mode from each state with each basis set can be found in Table S6.

Supporting Table 1: Summary of simulation systems, including the X-ray structure on which they are based, and the numbers of amino acids, solute atoms, water molecules, and counter-ions.

Simulation System	X-ray Structure	Number of Amino acids	Water Molecules	Na^+	Cl^-	Substrate Atoms
GTP			2595	9	5	45
$GTP \cdot Mg^{2+}$			3043	9	7	45
$Ras \cdot GTP \cdot Mg^{2+}$ Open	1QRA	1-166	21882	61	61	2674
$Ras \cdot GTP \cdot Mg^{2+}$ Closed	1QRA	1-166	21884	61	61	2674
$Ras \cdot GTP \cdot Mg^{2+} \cdot RasGAP$	1WQ1	1-166 / 714-1047	58058	162	162	7856
$Ras \cdot GDP \cdot Mg^{2+} \cdot P_i \cdot RasGAP$	1WQ1	1-166 / 714-1047	58056	162	162	7854
$Ras \cdot GDP \cdot Mg^{2+}$	4Q21	1-168	21851	61	61	3009

Supporting Table 2: All vibrational modes calculated for all of the six snapshots for each simulated state.

Supporting_Table_2.xls (separate file download)

Supporting Table 3: Partial charges: The ESP partial charges were calculated every 0.25 fs from 0.5 ps QM/MM simulations. The atoms of the triphosphate the Mg^{2+} and its coordinating partners are treated quantum mechanically. For each atom of the quantum region, we determined an average partial charge over the 2,000 values of the trajectory for one snapshot. The relative errors of these values are about 10%. The values for each atom of one snapshot were then averaged over the six different snapshots for one state. The average charges of the atoms were summed according to their functional groups as categorized in Figure S5. All values are given in the unit of the elementary charge, e_0. A detailed list of all values can be found in Table S4.

	GTP	$GTP \cdot Mg^{2+}$	$Ras \cdot GTP\ Mg^{2+}$	$Ras \cdot GTP \cdot Mg^{2+}$ $\cdot GAP$	Intermediate	$Ras \cdot GDP \cdot Mg^{2+}$
Methyl	0.27	0.23	0.15	0.02	0.11	0.16
$P\alpha$	-0.92	-0.80	-0.98	-0.80	-0.93	-1.02
$P\beta$	-1.65	-1.64	-1.37	-1.46	-1.82	-1.90
$P\gamma$	-1.70	-1.46	-1.43	-1.39	-1.02	
Mg^{2+}		1.50	1.51	1.25	1.33	1.64
HOH		0.16	-0.06	0.07	0.03	-0.01
Ser17			0.11	0.18	0.17	0.13
Thr35			0.07	0.13	0.12	
P3	1.34	1.36	1.43	1.46	1.56	
P2	1.33	1.34	0.77	0.91	1.03	1.08
O32	-0.52	-0.61	-0.47	-0.53	-0.72	-0.88
O23	-1.01	-0.88	-0.83	-0.86		
O22	-0.93	-0.86	-0.60	-0.61	-0.86	-0.84
O33	-1.04	-0.99	-1.0	-0.99		
O13	-0.99	-0.95	-0.99	-1.00		
O12	-0.92	-0.91	-0.88	-0.89	-0.92	-0.95
O31	-0.61	-0.60	-0.18	-0.34	-0.35	-0.31

Supporting Table 4: All partial charges of each atom calculated for all of the six snapshots for each simulated state.

Supporting_Table_4.xls (separate file download)

Supporting Table 5: Partial charges without Mg^{2+} in the QM box. The ESP partial charges were calculated every 0.25 fs from 0.5 ps QM/MM simulations. The atoms of the triphosphate are treated quantum mechanically. For each atom of the quantum region, we determined an average partial charge over the 2,000 values of the trajectory for one snapshot. The relative errors of these values are about 10%. The values for each atom of one snapshot were then averaged over the six different snapshots for one state. The average charges of the atoms were summed according to their functional groups as categorized in Fig. 2. All values are given in the unit of the elementary charge, e_0.

	GTP	GTP·Mg^{2+}	Ras·GTP·Mg^{2+}	Ras·GTP·Mg^{2+} ·RasGAP	Intermediate
Methyl	0.27	0.21	0.13	-0.06	0.10
Pα	-0.92	-0.90	-1.07	-0.80	-0.99
Pβ	-1.65	-1.68	-1.53	-1.62	-1.97
Pγ	-1.70	-1.64	-1.54	-1.52	-1.14

Supporting Table 6: Comparison of the results from instantaios normal mode analysis for all simulated states with the basis sets of 6-31G*, 6-31++G** and 6-311++G**.
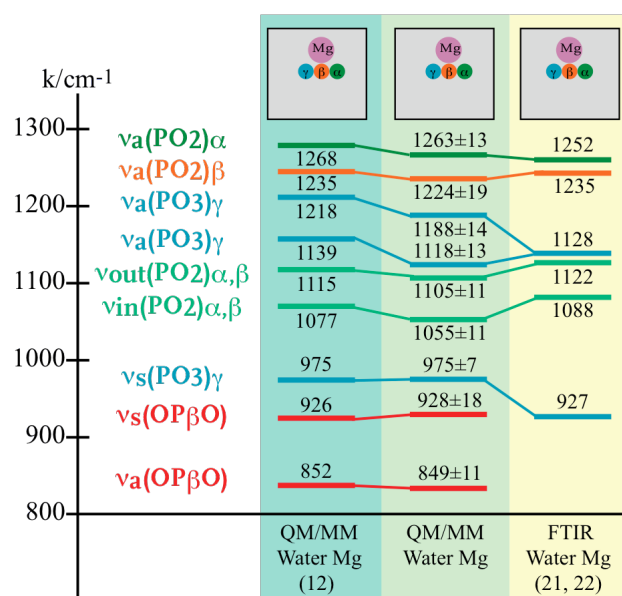
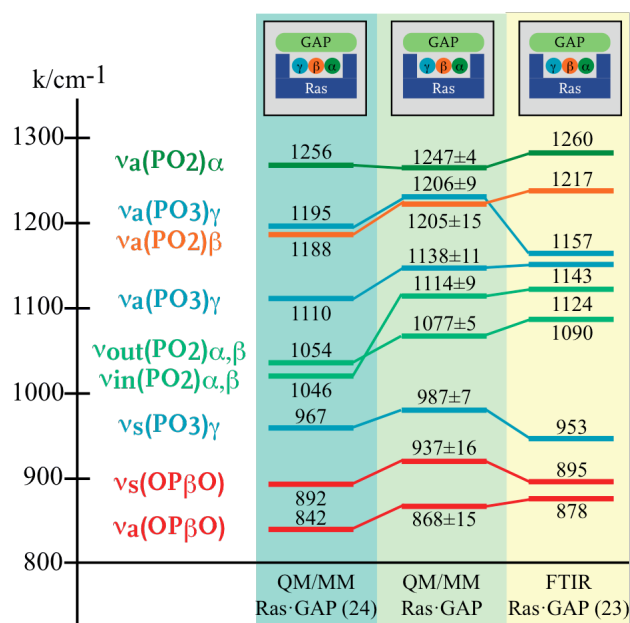*Supporting_Table_6.xls (separate file download)*
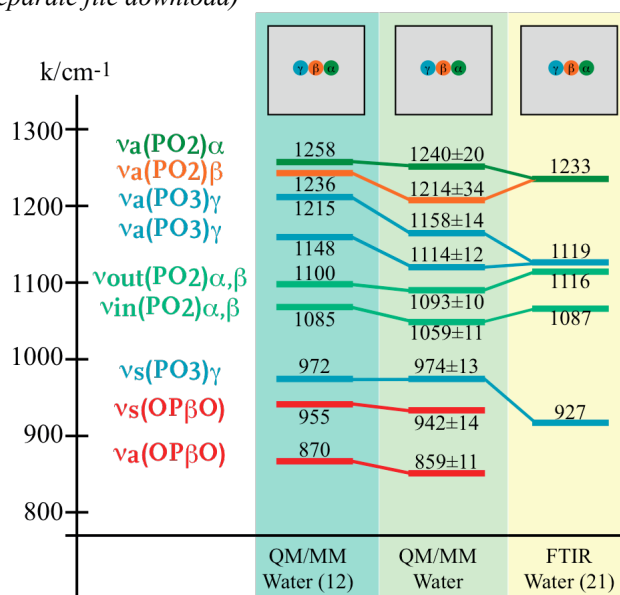
Supporting Figure 1: Comparison of calculated and measured vibrational modes of GTP in water. The calculated vibrational modes from Fei *et al.* (12) are shaded in light blue, our results are shaded in light green, and the measured vibrational modes of Wang *et al.* (21) are shaded in light yellow.
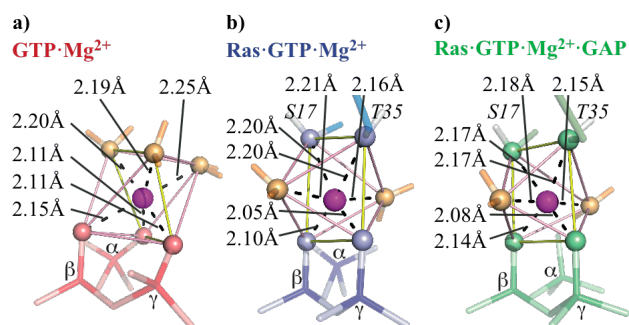
Supporting Figure 2: Coordination sphere of the magnesium ion in a) water, b) Ras and c) Ras·GAP. The distances are averaged values of six separate, 0.5 ps equilibrium QM/MM simulations for each shown state. Already small changes in the coordination and distance of the Mg^{2+} affect the spectral features and the charge distribution of the triphosphate.


Supporting Figure 3: Comparison of calculated and measured vibrational modes for GTP with Mg^{2+} in water. The calculated vibrational modes from Fei *et al.* (12) are shaded in light blue, our results are shaded in light green, and the measured vibrational modes of Wang *et al.* (21) and Takeuschi *et al.* (22) are shaded in light yellow.

Supporting Figure 4: Comparison of calculated and measured vibrational modes for Ras·GTP·Mg^{2+} ·RasGAP in water. The calculated vibrational modes from te Heesen *et al.* (24) are shaded in light blue, our results are shaded in light green, and the measured vibrational modes of Allin *et al.* (23) are shaded in light yellow.
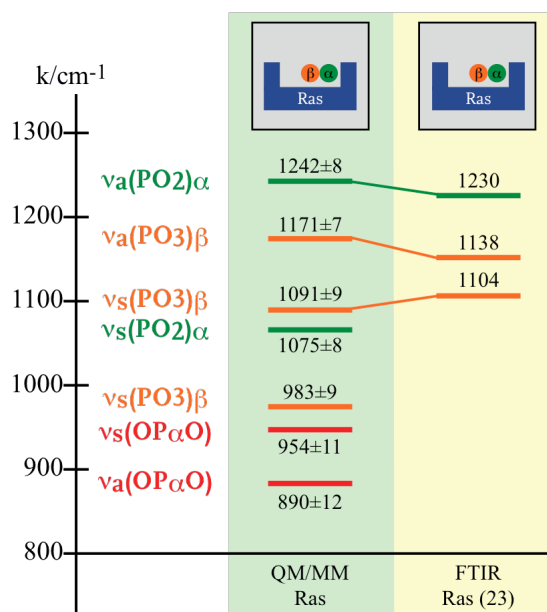
Supporting Figure 5: Comparison of calculated and measured vibrational modes for Ras·GDP·Mg^{2+} in water. Our results are shaded in light green, and the measured vibrational modes of Allin *et al.* (23) are shaded in light yellow.
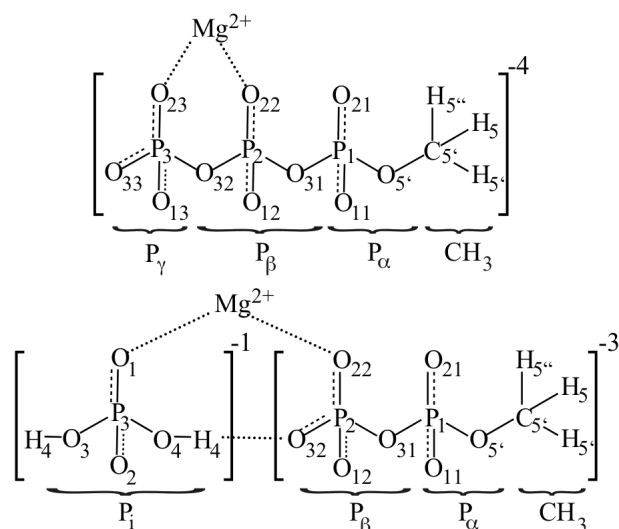
Supporting Figure 6: Atom names and functional groups of the phosphate regions. The atoms are categorized in functional groups regarding the charge distribution. In total there are five different phosphate groups: The γ-phosphate (consisting of the atoms: O_{13}, O_{23}, O_{33} and P_3) or the P_i (O_1, O_2, O_3, O_4, H_3, H_4 and P_3) in the intermediate state, the β-phosphate (O_{12}, O_{22}, O_{32}, O_{31} and P_2), the α-phosphate (O_{11}, O_{21}, $O_{5'}$ and P_1), and the methyl group (H_5, $H_{5'}$, $H_{5''}$ and $C_{5'}$), where H_5 is a dummy atom at the junction between the QM and the MM regions.

Supporting References

1.   Scheidig, A. J., C. Burmester, and R. S. Goody. 1999. The pre-hydrolysis state of p21(ras) in complex with GTP: new insights into the role of water molecules in the GTP hydrolysis reaction of ras-like proteins. Struct. Fold. Des. 7:1311-1324.

2.   Scheffzek, K., M. R. Ahmadian, W. Kabsch, L. Wiesmuller, A. Lautwein, F. Schmitz, and A. Wittinghofer. 1997. The Ras-RasGAP complex: structural basis for GTPase activation and its loss in oncogenic Ras mutants. Science 277:333-338.

3.   Milburn, M. V., L. Tong, A. M. Devos, A. Brunger, Z. Yamaizumi, S. Nishimura, and S. H. Kim. 1990. Molecular Switch for Signal Transduction - Structural Differences between Active and Inactive Forms of Protooncogenic Ras Proteins. Science 247:939-945.

4.   Höweler, U. 2007. MAXIMOBY In CHEOPS, Altenberge, Germany.

5.   Hess, B., C. Kutzner, D. van der Spoel, and E. Lindahl. 2008. GROMACS 4: Algorithms for highly efficient, load-balanced, and scalable molecular simulation. J Chem Theory Comput 4:435-447.

6.   Van der Spoel, D., E. Lindahl, B. Hess, G. Groenhof, A. E. Mark, and H. J. C. Berendsen. 2005. Gromacs: Fast, Flexible, and Free. J Comput Chem 26:1701-1718.

7.   Jorgensen, W. L., D. S. Maxwell, and J. TiradoRives. 1996. Development and testing of the OPLS all-atom force field on conformational energetics and properties of organic liquids. Journal of the American Chemical Society 118:11225-11236.

8.   Jorgensen, W. L., and J. D. Madura. 1985. Temperature and Size Dependence for Monte-Carlo Simulations of Tip4p Water. Molecular Physics 56:1381-1392.

9.   Darden, T., D. York, and L. Pedersen. 1993. Particle Mesh Ewald - an N.Log(N) Method for Ewald Sums in Large Systems. Journal of Chemical Physics 98:10089-10092.

10.   Bussi, G., D. Donadio, and M. Parrinello. 2007. COMP 8-Canonical sampling through velocity rescaling. Abstr Pap Am Chem S 234.

11.   Parrinello, M., and A. Rahman. 1981. Polymorphic Transitions in Single-Crystals - a New Molecular-Dynamics Method. J Appl Phys 52:7182-7190.

12.   Xia, F., T. Rudack, C. Kötting, J. Schlitter, and K. Gerwert. 2011. The specific vibrational modes of GTP in solution and bound to Ras: a detailed theoretical analysis by QM/MM simulations. Phys Chem Chem Phys 13:21451-21460.

13.   Frisch, M. J., G. W. Trucks, H. B. Schlegel, G. E. Scuseria, M. A. Robb, J. R. Cheeseman, J. J. A. Montgomery, T. Vreven, K. N. Kudin, J. C. Burant, J. M. Millam, S. S. Iyengar, J. Tomasi, V. Barone, B. Mennucci, M. Cossi, G. Scalmani, N. Rega, G. A. Petersson, H. Nakatsuji, M. Hada, M. Ehara, K. Toyota, R. Fukuda, J. Hasegawa, M. Ishida, T. Nakajima, Y. Honda, O. Kitao, H. Nakai, M. Klene, X. Li, J. E. Knox, H. P. Hratchian, J. B. Cross, C. Adamo, J. Jaramillo, R. Gomperts, R. E. Stratmann, O.

Yazyev, A. J. Austin, R. Cammi, C. Pomelli, J. W. Ochterski, P. Y. Ayala, K. Morokuma, G. A. Voth, P. Salvador, J. J. Dannenberg, V. G. Zakrzewski, S. Dapprich, A. D. Daniels, M. C. Strain, O. Farkas, D. K. Malick, A. D. Rabuck, K. Raghavachari, J. B. Foresman, J. V. Ortiz, Q. Cui, A. G. Baboul, S. Clifford, J. Cioslowski, B. B. Stefanov, G. Liu, A. Liashenko, P. Piskorz, I. Komaromi, R. L. Martin, D. J. Fox, T. Keith, M. A. Al-Laham, C. Y. Peng, A. Nanayakkara, M. Challacombe, P. M. W. Gill, B. Johnson, W. Chen, M. W. Wong, C. Gonzalez, and J. A. Pople. 2003. Gaussian 03. Gaussian Inc., Pittsburgh PA.

14.   Groenhof, G., M. Bouxin-Cademartory, B. Hess, S. P. De Visser, H. J. C. Berendsen, M. Olivucci, A. E. Mark, and M. A. Robb. 2004. Photoactivation of the photoactive yellow protein: Why photon absorption triggers a trans-to-cis lsomerization of the chromophore in the protein. Journal of the American Chemical Society 126:4228-4233.

15.   CPMD. http://www.cpmd.org/, Copyright IBM Corp 1990-2008, Copyright MPI für Festkörperforschung Stuttgart 1997-2001.

16.   Biswas, P. K., and V. Gogonea. 2005. A regularized and renormalized electrostatic coupling Hamiltonian for hybrid quantum-mechanical-molecular-mechanical calculations. Journal of Chemical Physics 123.

17.   Becke, A. D. 1988. Density-Functional Exchange-Energy Approximation with Correct Asymptotic-Behavior. Phys Rev A 38:3098-3100.

18.   Perdew, J. P. 1986. Density-Functional Approximation for the Correlation-Energy of the Inhomogeneous Electron-Gas. Phys Rev B 33:8822-8824.

19.   Hartwigsen, C., S. Goedecker, and J. Hutter. 1998. Relativistic separable dual-space Gaussian pseudopotentials from H to Rn. Phys Rev B 58:3641-3662.

20.   Singh, U. C., and P. A. Kollman. 1984. An approach to computing electrostatic charges for molecules. J Comput Chem 5:129-145.

21.   Wang, J. H., D. G. Xiao, H. Deng, R. Callender, and M. R. Webb. 1998. Vibrational study of phosphate modes in GDP and GTP and their interaction with magnesium in aqueous solution. Biospectroscopy 4:219-227.

22.   Takeuchi, H., H. Murata, and I. Harada. 1988. Interaction of Adenosine 5'-Triphosphate with Mg-2+ - Vibrational Study of Coordination Sites by Use of O-18-Labeled Triphosphates. Journal of the American Chemical Society 110:392-397.

23.   Allin, C., M. R. Ahmadian, A. Wittinghofer, and K. Gerwert. 2001. Monitoring the GAP catalyzed H-Ras GTPase reaction at atomic resolution in real time. Proc. Natl. Acad. Sci. U.S.A. 98:7754-7759.

24.   te Heesen, H., K. Gerwert, and J. Schlitter. 2007. Role of the arginine finger in Ras-RasGAP revealed by QM/MM calculations. FEBS Lett. 581:5677-5684.

25.   Rudbeck, M. E., S. Kumar, M. A. Mroginski, S. O. N. Lill, M. R. A. Blomberg, and A. Barth. 2009. Infrared Spectrum of Phosphoenol Pyruvate: Computational and Experimental Studies. J Phys Chem A 113:2935-2942.

26.   Allin, C., and K. Gerwert. 2001. Ras catalyzes GTP hydrolysis by shifting negative charges from gamma- to beta-phosphate as revealed by time-resolved FTIR difference spectroscopy. Biochemistry-Us 40:3037-3046.